# Modelling the UV and Optical Emission from Accretion Disks around Supermassive Black Holes

PHYS6006 Progress Report

**Alexander S. Weston**

Supervisor: Professor Ian M. M$^{c}$Hardy

January 4, 2021

**Abstract**

The origin of UV/optical variability observed in active galactic nuclei is currently a mystery. Although the general consensus is that the majority of this variability is likely caused by x-ray reprocessing, there is currently not sufficient evidence to confirm this as fact. Dependent on our findings, this project aims to provide evidence for or against this hypothesis. So far, our modelling has generated realistic temperature profiles and disk spectrums for both the illuminated and non-illuminated cases. Response functions for the x-rays have been generated for a face-on disk after we considered the effects of optical depth upon x-ray reprocessing. Our next steps are to create response functions for inclined disks. We will then use these response functions for convolution with real x-ray data to determine the accuracy of the model by comparing these results with real UV/optical data from the same galaxy that the x-ray data was taken from, NGC 4593. The project is currently on track to be completed on time.

# 1 Introduction

## 1.1 Theoretical Background

Active galactic nuclei (AGN) have been studied in depth since at least the 1960's [1]. It has been reasoned for a long time that AGN we observe across the universe are powered by accretion onto supermassive black holes [2], one of the most efficient matter to energy conversion processes in the universe. Most AGN emit across the electromagnetic spectrum from radio to gamma rays [3]. One of the key areas of modern AGN research relates to their observed UV/optical variability [4]. There are currently two leading theories to the origin of this variability. One of these suggestions is that the variability originates in variations in the inflow of accretion material [5]. The second suggestion is that a variable x-ray corona illuminates the disk which heats it causing it to re-radiate [6].

Most current work on AGN relies on either of two models to describe the temperature profile of the disk. The first, known as the Shakura-Sunyaev (SS) model after the authors [7], is a Newtonian optically thick but geometrically thin model which describes the transfer of potential energy to thermal energy as material falls towards the black hole due to friction in the disk. The second, by Novikov and Thorne [8], is a relativistic generalisation of the SS model. Most have used the former due to the vastly simpler mathematics involved.

## 1.2 Aims and Objectives of the Project

With this project, we aim to accurately model the UV/optical variability observed in AGN and determine the origin of such variability. We follow a similar line of work to that in [4, 9]. We hypothesise that the variability in the disk emission can be explained via an x-ray reprocessing model and we seek to test the accuracy of this model. We can perform this test by comparing lags between x-ray and UV/optical data and seeing if they match up to x-ray data convolved with a response function we generate based on the geometry of the AGN. If we get a successful match, we can use the lags between x-ray and UV/optical emissions to map and determine the size of the AGN region around the black hole with reasonable accuracy - a technique known as reverberation mapping [10].

## 1.3 Method - Fundamental Equations and Applications

### 1.3.1 Disk Temperature Profile

A lot of the mathematics in this section involving non-illuminated accretion disks is aided by large parts of [11]. The SS model produces a temperature profile of the disk $T(R)$ given by

$$T(R) = \left(\frac{3GM\dot{M}}{8\pi\sigma_{SB}R^3}\left(1-\left(\frac{R_{in}}{R}\right)^{1/2}\right)\right)^{1/4}, \tag{1}$$

where $M$ is the mass of the black hole, $\dot{M}$ is the mass accretion rate, $R$ is the radial distance from the centre of the black hole, $R_{in}$ is the inner radius of the disk, $G$ is the gravitational constant and $\sigma_{SB}$ is the Stefan-Boltzmann constant. Here we have assumed that the disk radiates like a black body (BB). The factor of $1-\left(\frac{R_{in}}{R}\right)^{1/2}$ has a very important effect upon the temperature profile at the inner sections of the disk and cannot be ignored, despite its negligible effect upon the overall disk spectrum as we show in figures (1) and (2). To help with comparing different AGN, it is often convenient to use a system of units where we measure radii in gravitational radii $R_g$, mass in solar masses $M_\odot$ and the accretion rate in Eddington units $\dot{m}$. Using the change of variables

$$R = rR_g = r\frac{GM}{c^2}, \tag{2}$$

$$M = mM_\odot, \tag{3}$$

$$\dot{M} = \dot{m}\dot{M}_{Edd} = \dot{m}\frac{L_{Edd}}{\eta c^2} = \dot{m}\frac{4\pi GMm_p}{\eta c\sigma_T}, \tag{4}$$

we obtain a new temperature profile $T(r)$ given by

$$T(r) = \left(\frac{3m_pc^5\dot{m}}{2\eta\sigma_T\sigma_{SB}GM_\odot mr^3}\left(1-\left(\frac{r_{in}}{r}\right)^{1/2}\right)\right)^{1/4}, \tag{5}$$

where $m_p$ is the proton mass, $c$ is the speed of light in a vacuum, $\eta$ is the accretion efficiency given by (6) and $\sigma_T$ is the Thomson cross-section. The accretion efficiency is given by

$$\eta = 1 - \sqrt{1 - \frac{2r}{3r_{in}}}. \tag{6}$$

We calculate $r_{in}$ by using the black hole's dimensionless spin parameter $a$. The formulae for $r_{in}(a)$ are quite complex so we do not replicate them here.[1] Some crucial values of $r_{in}$ are 1, 6, and 9 $R_g$ for $a = 1$, 0 and -1 respectively.[2] A positive value of $a$ indicates black hole spin is in the same direction as the rotation of the accretion disk. Most supermassive black holes have $a$ in the range 0.5-1 [15].

We have chosen to model our x-ray corona as a point-source of luminosity $L_X$ at a height $H_X$ above the accretion disk. This is known as the *lamp post* model [4]. This vastly simplifies the mathematics involved when compared to a realistic, spherical shape without compromising accuracy.[3] The x-ray source has the effect of adding energy to the disk and heating it. This effect can be modelled by giving the disk a new effective temperature $T_{new}(r)$ given by

$$T_{new}(R) = \left(T^4(R) + \frac{L_X(1-A)H_X}{4\pi\sigma_{SB}(H_X^2 + R^2)^{3/2}}\right)^{1/4}, \tag{7}$$

with $A$ the disk albedo. After applying the same change of variables as previous in addition to

$$H_X = h_X R_g, \tag{8}$$

we produce our final result

$$T_{new}(r) = \left(\frac{3m_p c^5 \dot{m}}{2\eta\sigma_T\sigma_{SB}GM_\odot m r^3}\left(1 - \left(\frac{r_{in}}{r}\right)^{1/2}\right) + \frac{L_X(1-A)c^4 h_X}{4\pi\sigma_{SB}G^2M_\odot^2 m^2(h_X^2 + r^2)^{3/2}}\right)^{1/4}. \tag{9}$$

A derivation of the extra term in equation (9) due to x-ray reprocessing can be found in [4].

#### 1.3.2 Disk Spectrum

A BB spectrum is described by the Planck formula

$$B_\nu(T) = \frac{2h\nu^3}{c^2}\frac{1}{\exp\left(\frac{h\nu}{k_BT}\right) - 1}, \tag{10}$$

with $h$ the Planck constant, $k_B$ the Boltzmann constant and $\nu$ the frequency. By considering $B_\nu(T(r))$, one can calculate the overall disk spectrum $L_\nu$ by integrating over all radii

$$L_\nu = 2\pi\int_{r_{in}}^{r_{out}} B_\nu(T(r))2\cdot 2\pi r\left(\frac{GM_\odot m}{c^2}\right)^2 dr, \tag{11}$$

where the first factor of $2\pi$ comes from integration over half of physical space, the second 2 comes from two sides of the disk and the final $2\pi$ comes from an infinitesimal thickness ring area element on the disk.

#### 1.3.3 Tools and Basics of Model

To perform our calculations, we have used *Spyder* 3.31 for *Python* 3.7 which allowed us to use *Numpy* for number manipulation. This has allowed us to perform numerical work efficiently. For integration, we have opted to use *Simpson's rule*. This is similar to the more well-known *trapezium rule* but is slightly more accurate. To model our accretion disk, we have divided the disk into 1000 logarithmically-spaced segments,[4] across which we approximate both $T$ and $T_{new}$ as constant. This was done as the inner disk is the region producing the most amount of flux and has the greatest variability in $T(r)$. The outer parts of the disk vary, relatively, very little in temperature so can be made larger to allow us for more segments further in. To test the accuracy of our calculations and theory, routine integrations of plotted functions have been performed to ensure that the area under said functions are equal.

[1] A curious reader can find them as equations (2.21) in [12].

[2] A black hole with $a = 0$ is known as a Schwarzchild black hole [13] and a black hole with $a = 1$ is known as a fully-Kerr black hole [14].

[3] For an example analysis using a spherical x-ray source, see [16].

[4] i.e. described by a geometric progression.

# 2 Progress so Far

## 2.1 Disk Profiles

Our first task was to produce temperature profiles and disk spectrums for both the non-illuminated and illuminated disks. The latter has a very distinctive shape [11] which can be used to form a strong foundation to test the accuracy of our calculations. Our results are shown in figures (1) and (2).

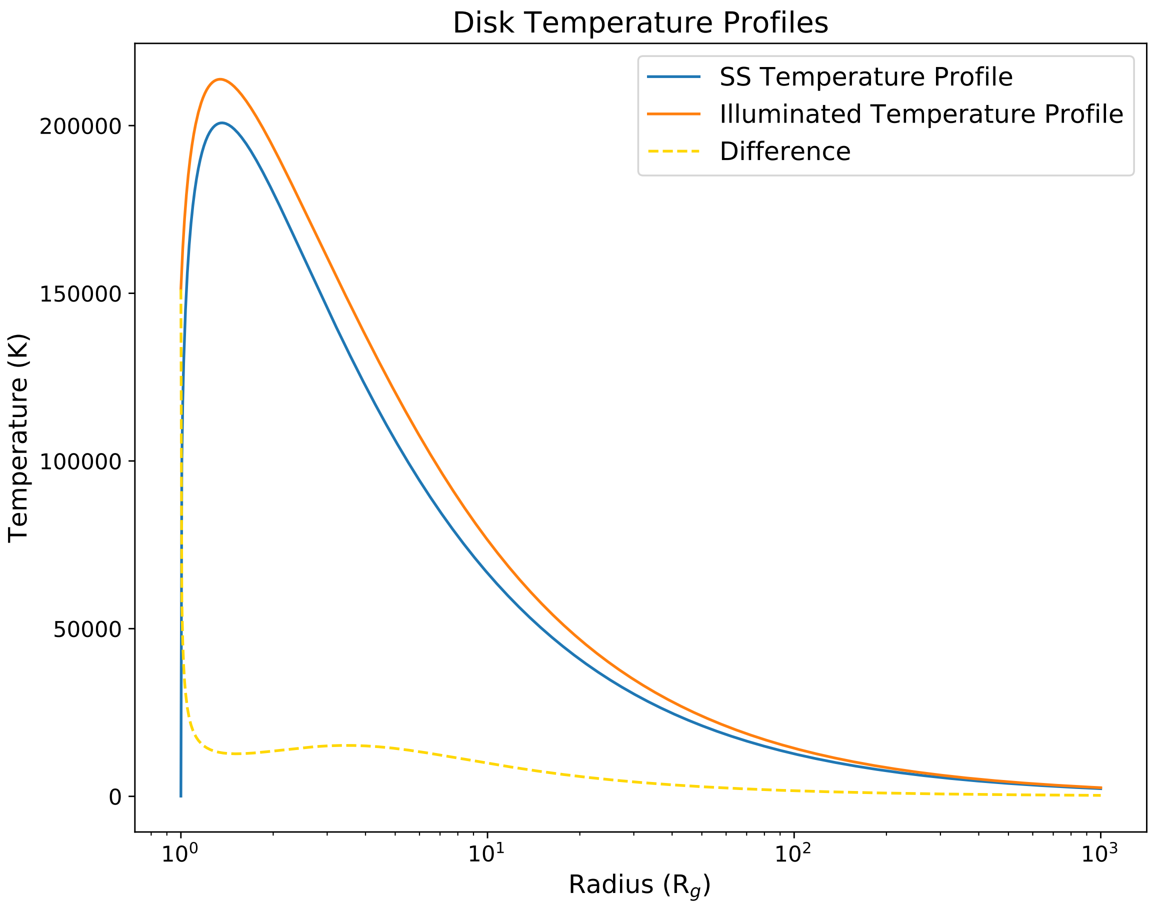


Figure 1: The temperature profiles for an example black hole and their difference. The plot uses $m = 5\text{x}10^7$, $\dot{m} = 0.05$, $r_{out} = 10^3$, $a = 1$, $L_X = 8\text{x}10^{10}\ L_\odot$, $h_X = 3$ and $A = 0.3$. These values are similar to a "typical" AGN such as NGC 4593 [17]. Clearly the illuminated disk is hotter as one would expect given the extra energy being added to the disk. The importance of the $1 - \left(\frac{r_{in}}{r}\right)^{1/2}$ term is clearly displayed in the SS profile as $T(r)$ approaches 0 as $r$ approaches $r_{in}$. Without this term, the temperature would be substantially larger at small radii and not produce the response functions in (3).

## 2.2 Response Functions

### 2.2.1 Calculation

The next part of the project was to calculate response functions for our accretion disk. This is physically equivalent to an instantaneous pulse of x-ray emission travelling from the centre of the x-ray source and hitting the disk which re-emits it as BB radiation. This re-emission happens over a period of time which is a function of the size of the accretion disk. To simplify the mathematics, we first consider the face-on disk. We can then describe the

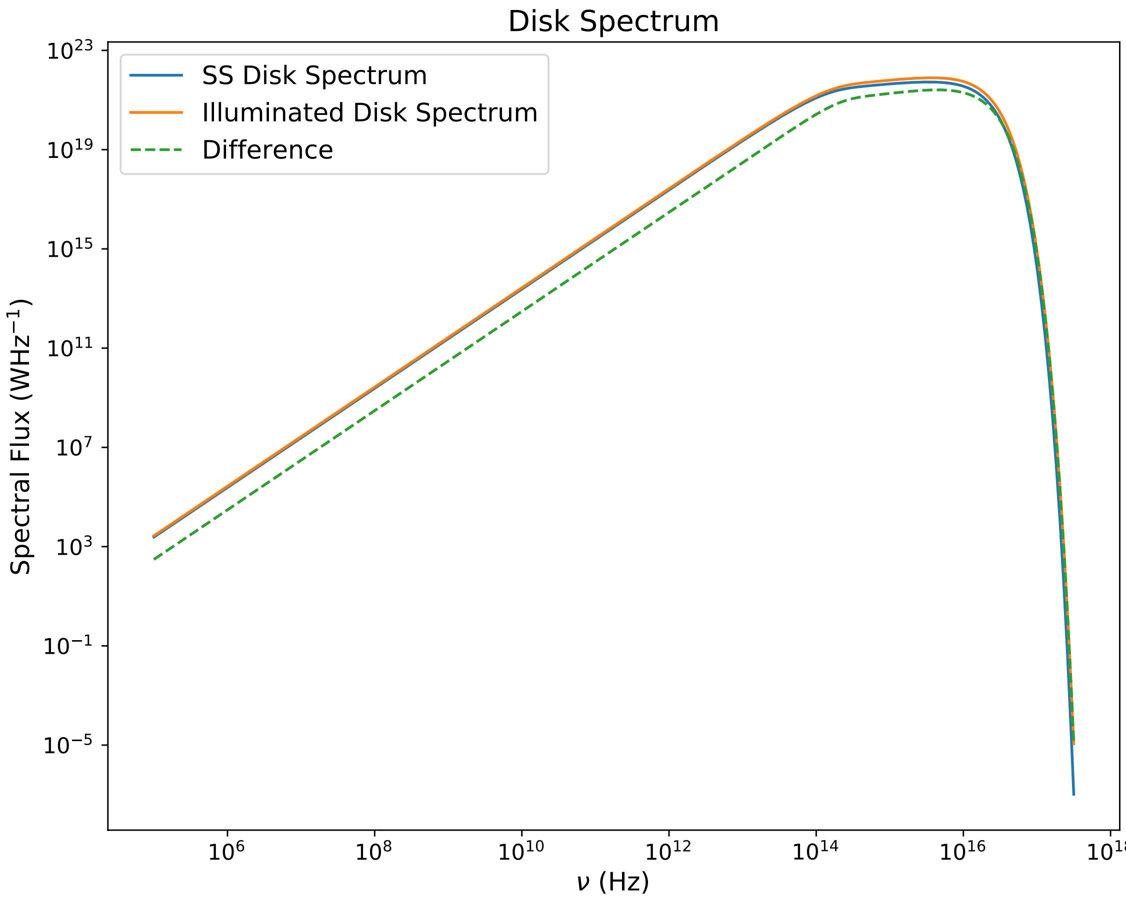


Figure 2: The spectrum of the two temperature profiles used in figure (1) and their difference. The distinctive three-section shape is clearly visible in the plot. At lower frequencies, the spectral flux grows as $\nu^2$ before transitioning to $\nu^{1/3}$ and then to $\nu^2 \exp\left(-\frac{h\nu}{k_B T}\right)$ [11]. The peak of the spectrum lies in the UV and is often referred to as the *big blue bump* in the literature [18].

wave of illumination as a function of radial coordinate of the disk only. We calculate the response function as follows. We sample radii in the disk and calculate the area elements at these radii. We then multiply this by the difference between our two BB functions $B_\nu(T_{new}(r)) - B_\nu(T(r))$ as well as calculating the lag $\tau(r)$. The lag is the time difference we observe on Earth between the x-rays and re-processed light from the disk. For a face-on disk, $\tau(r) = \frac{GM_\odot m}{c^2}\frac{h_X+\sqrt{h_X^2+r^2}}{c}$.[5] The response function is then divided by the difference of the upper and lower limits of lag at each segment.[6] We can then repeat this for any frequency within a given $\nu_l$ and $\nu_h$ and then integrate over these individual response functions. This creates a response function comparable with data from a space telescope. Throughout this calculation, one must be careful to avoid normalising the data at any point as doing so loses important information about the size of the response function, preventing direct comparison between different response functions. One verification method we applied involved calculating response functions for various frequency ranges. We would expect for lower frequencies that the peak of the response function would be at a later time than one for a higher frequency. This is because once outside the peak disk temperature radius, the temperature quickly falls off. Then, by Wein's Law, one can show that the peak wavelength of emission should

[5] i.e. light travels from our point source to the disk and back in the direction of Earth.

[6] For the face-on disk this difference is $\tau(r+\delta r) - \tau(r)$ with $\delta r$ the thickness of the segment. In the limit $\delta r \to 0$ we obtain the differential $\frac{\partial L_{diff}}{\partial \tau}$ as our response function.

follow it. This behaviour was observed in our results, being a strong indicator of the mathematical footing of our calculations.

### 2.2.2 Issues Encountered and Methods to Resolve

Our initial response functions were nonphysical and displayed a "banana" shape. This has not been observed in any other response functions we could find in the literature (see for example [9, 19]). The shape one would expect would be a rise to a peak then a fall, very similar in shape to the SS temperature profile in figure (1). The initial rise is due to the area elements of the disk increasing in size with radius whilst the later fall is due to the $1/r^2$ behaviour of point-source emission. After a thorough investigation, the cause was found to be due to the temperature differences at small radii due to our BB assumption. Hence we had to adapt our model, first finding a physical justification for an adaption. We found the theory of advection-dominated accretion flows solved this (for more on ADAF, see [20]). Although the physics is quite complex, the general effect is comparable to a lower efficiency of re-processing than is predicted. From this, we were able to justify an optical depth adaptation at lower radii, reducing the extreme, nonphysical, temperature difference displayed at these radii. The simplest accurate adaptation we could perform was modelling optical depth which previously had not been considered. [11] provided us with a reasonable equation which we could use to approximate the change in optical depth at smaller radii. We were able to physically justify this by the disk "blooming" near to the black hole where the thin disk approximation is less valid. As it blooms, its density and optical depth decreases. By approximating the change via classical radiative transfer equations we can perform the following substitution in equation (9)

$$L_X \to L_X(1 - \exp(-\chi)), \tag{12}$$

with $\chi$ our optical depth defined as

$$\chi = \chi_0 \left(1 - \left(\frac{r_{in}}{r}\right)^{1/2}\right)^{4/5}, \tag{13}$$

where $\chi_0$ is a constant of order 1 left as a free variable. Applying this substitution puts our response functions into the physically-plausible regime and has allowed us to begin the next steps of our work. Equation (13) was adapted from [11]. An example of response functions with and without optical depth modelling are provided in figure (3).

## 3 Future Work

Whilst we have completed the fundamental ground work in our project, we still have results to obtain. First, we need to generalise our response functions to inclined disks. Most accretion disks will be inclined when viewed from Earth [21]. To perform this calculation we must divide our disk into segments instead of rings and calculate the time delay at each segment. This calculation is substantially slower and if possible, optimisations will need to be found. During this calculation one must multiply the response function by a factor of $\cos i$ with $i$ the inclination of the disk.[7] One must also use a generalised lag function $\tau(r, \phi)$ as given by equation (3.3) in [4].

Once we have a successful method of generating response functions for any inclination, we will convolve them with our x-ray data from NGC 4593. This can be represented mathematically as

$$f(t) = \int_{\tau_l}^{\tau_h} \Psi(\tau) S_X(t - \tau)\, d\tau, \tag{14}$$

where $f(t)$ is our reprocessed light curve with $\Psi(\tau)$ our response function and $S_X(t)$ our x-ray light curve for minimum and maximum lags $\tau_l$ and $\tau_h$ respectively. Our $f(t)$ can then be directly compared with a real UV/optical light curve via a cross-correlation function (CCF) [4]. It may be necessary to use a more advanced CCF such as that given in [22], if our data is of poor quality with large errors. From this comparison, we will determine whether our model is accurate or requires improvement.

[7] $i = 0$ is for a face-on disk.

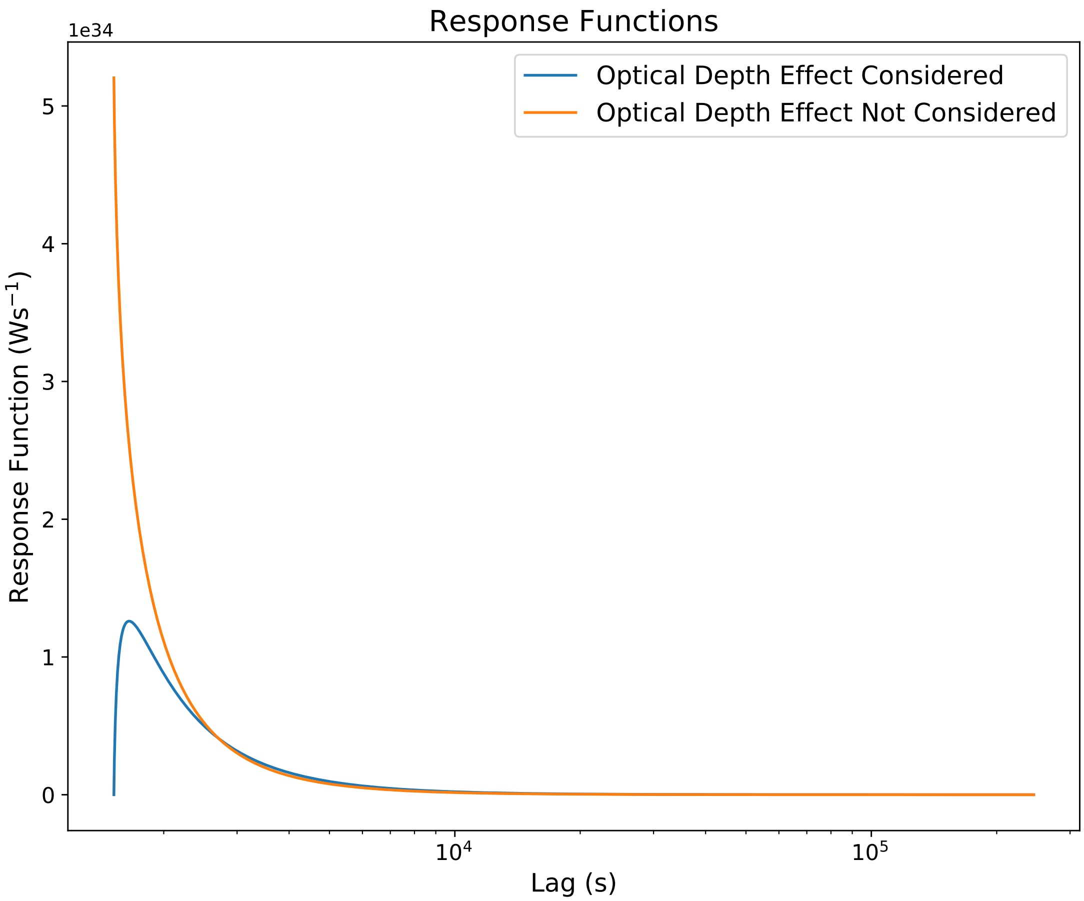


Figure 3: This plot shows the importance of considering optical depth upon our results. The orange line represents our original "banana-shaped" response function whilst the blue line represents our new, optical depth-considering, response function. This plot uses the same parameters as figures (1) and (2). We have used a frequency range of $10^5$-$10^{17.5}$ Hz. The effect of modelling optical depth is substantial over a very small lag range at small lags (corresponding for the face-on disk as close to the black hole) and negligible for larger lags. A lag of 0 would be when the x-rays which generated the plotted response function would be received by an observer on Earth. Considering optical depth generates a response function which agrees with those seen in academic papers such as [4, 9].

# 4 Conclusions

So far, we have successfully generated temperature profiles and spectrums for the SS and illuminated disk cases. We have also generated response functions for a face-on disk. Our next step is to generalise this to the inclined disk.[8] Once we have done this we will be able to convolve our response functions with real x-ray data taken from NGC 4593. The results of this will then be compared with real UV/optical data from the same galaxy via cross-correlation. Doing all of these steps will allow us to determine if the cause of UV/optical variability, a currently unsolved mystery in extra-galactic astronomy, can be explained with disk reprocessing of x-rays from a bright source near to the black hole. The project is currently on-track to complete all the tasks outlined above.

[8] i.e. $i \neq 0$

## References


[1] Matias Montesinos. Review: Accretion Disk Theory. *arXiv e-prints*, art. arXiv:1203.6851, March 2012.

[2] D. Lynden-Bell. Galactic Nuclei as Collapsed Old Quasars. *Nature*, 223(5207):690–694, August 1969. doi: 10.1038/223690a0.

[3] C. D. Impey. *Active Galactic Nuclei Across the Electromagnetic Spectrum*, pages 685–686. Springer Netherlands, Dordrecht, 1994. ISBN 978-94-011-0794-5. doi: 10.1007/978-94-011-0794-5_111.

[4] Duncan Cameron. The relationship between uv and optical variability and x-ray variability in active galactic nuclei, thesis for the degree of doctor of philosophy. February 2014.

[5] P. Arévalo and P. Uttley. Investigating a fluctuating-accretion model for the spectral-timing properties of accreting black hole systems. *MNRAS*, 367(2):801–814, April 2006. doi: 10.1111/j.1365-2966.2006.09989.x.

[6] F. Haardt and L. Maraschi. A Two-Phase Model for the X-Ray Emission from Seyfert Galaxies. *ApJ*, 380: L51, October 1991. doi: 10.1086/186171.

[7] N. I. Shakura and R. A. Sunyaev. Black Holes in Binary Systems: Observational Appearances. In H. Bradt and Riccardo Giacconi, editors, *X-Ray and Gamma-Ray Astronomy*, volume 55, page 155, January 1973.

[8] I. D. Novikov and K. S. Thorne. Astrophysics of black holes. In *Black Holes (Les Astres Occlus)*, pages 343–450, January 1973.

[9] Edward M. Cackett, Keith Horne, and Hartmut Winkler. Testing thermal reprocessing in active galactic nuclei accretion discs. *MNRAS*, 380(2):669–682, September 2007. doi: 10.1111/j.1365-2966.2007.12098.x.

[10] R. D. Blandford and C. F. McKee. Reverberation mapping of the emission line regions of Seyfert galaxies and quasars. *ApJ*, 255:419–439, April 1982. doi: 10.1086/159843.

[11] Juhan Frank, Andrew R King, and Derek J Raine. *Accretion Power in Astrophysics*. Cambridge Univ. Pr, 3 edition, 1985. ISBN 9780521245302.

[12] James M. Bardeen, William H. Press, and Saul A. Teukolsky. Rotating Black Holes: Locally Nonrotating Frames, Energy Extraction, and Scalar Synchrotron Radiation. *ApJ*, 178:347–370, December 1972. doi: 10.1086/151796.

[13] K. Schwarzschild. On the Gravitational Field of a Mass Point According to Einstein's Theory. *Abh. Konigl. Preuss. Akad. Wissenschaften Jahre 1906,92, Berlin,1907*, 1916:189–196, January 1916.

[14] Roy P. Kerr. Gravitational Field of a Spinning Mass as an Example of Algebraically Special Metrics. *PRL*, 11 (5):237–238, September 1963. doi: 10.1103/PhysRevLett.11.237.

[15] Eugenie Samuel Reich. Spin rate of black holes pinned down. *Nature*, 500:135–135, 08 2013. doi: 10.1038/500135a.

[16] L. Ducci, S. Mereghetti, K. Hryniewicz, A. Santangelo, and P. Romano. Exploring the role of X-ray reprocessing and irradiation in the anomalous bright optical outbursts of A0538-66. *A&A*, 624:A9, April 2019. doi: 10.1051/0004-6361/201834390.

[17] Kelly D. Denney, Misty C. Bentz, Bradley M. Peterson, Richard W. Pogge, Edward M. Cackett, Matthias Dietrich, Jeffrey K. J. Fogel, Himel Ghosh, Keith D. Horne, Charles Kuehn, Takeo Minezaki, Christopher A. Onken, Vladimir I. Pronik, Douglas O. Richstone, Sergey G. Sergeev, Marianne Vestergaard, Matthew G. Walker, and Yuzuru Yoshii. The Mass of the Black Hole in the Seyfert 1 Galaxy NGC 4593 from Reverberation Mapping. *ApJ*, 653(1):152–158, December 2006. doi: 10.1086/508533.

[18] Y. Y. Zhou, K. N. Yu, E. C. M. Young, J. M. Wang, and E. Ma. Statistical Properties of the Big Blue Bump in Active Galactic Nuclei. *ApJ*, 475(1):L9–L12, January 1997. doi: 10.1086/310451.

[19] R. A. Edelson and J. H. Krolik. The Discrete Correlation Function: A New Method for Analyzing Unevenly Sampled Variability Data. *ApJ*, 333:646, October 1988. doi: 10.1086/166773.

[20] G. S. Bisnovatyi-Kogan and R. V. E. Lovelace. Influence of Ohmic Heating on Advection-dominated Accretion Flows. *ApJ*, 486(1):L43–L46, September 1997. doi: 10.1086/310826.

[21] G. de Vaucouleurs. Maximum ellipticities and inclinations of galaxies. In *Bulletin of the American Astronomical Society*, volume 2, pages 308–309, September 1970.

[22] Tal Alexander. *Is AGN Variability Correlated with Other AGN Properties? ZDCF Analysis of Small Samples of Sparse Light Curves*, volume 218, page 163. 1997. doi: 10.1007/978-94-015-8941-3_14.